



# Concurrent Current and Voltage Regulated Buck–Boost Converter for Automotive LED Matrix Headlights

Jiho Moon , Jaeseong Lee, Khurram Javed, Jupyo Hong, and Jeongjin Roh , *Senior Member, IEEE*

**Abstract**—Automotive light-emitting diode (LED) matrix headlights require both high-power efficiency and stable control of individual LEDs. The proposed power converter uses a buck–boost converter and a concurrent current and voltage regulation circuit to increase the overall efficiency. Additionally, the proposed system requires only one small inductor instead of two large inductors in other designs. The reference voltage for the buck–boost converter was generated according to the number of turned-ON LEDs. Subsequently, for the optimum current regulation of the LED matrix headlight, the output voltage of the buck–boost converter follows the reference voltage. The main control circuit was fabricated on a chip using a 0.18- $\mu\text{m}$  BCD process for functional testing. The proposed system has an operating input voltage range of 7–60 V and an output voltage range of 1.05–60 V, depending on the number of LEDs. The proposed power system successfully demonstrated the individual control of LEDs for matrix headlights. Moreover, a dimming test was conducted to confirm that the brightness of the LEDs could be individually controlled.

**Index Terms**—Buck–boost converter, current regulation, light-emitting diode (LED) matrix, voltage regulation.

## I. INTRODUCTION

THE utilization of light-emitting diodes (LEDs) in lighting applications is becoming increasingly popular. This trend is attributed to their efficiency, fast response, longevity, and small form factor, which have resulted from recent advancements in their fabrication [1], [2]. Because of these benefits, various LED driving circuits have become important [3], [4], [5], [6], [7], [8]. Particularly, LEDs are increasingly being incorporated into automobiles, with all major lighting systems (such as headlights, brake lights, and turn signals) now being designed using

Manuscript received 20 July 2022; revised 17 November 2022 and 14 January 2023; accepted 5 February 2023. Date of publication 8 February 2023; date of current version 10 March 2023. This work was supported in part by the LX Semicon Corporation, South Korea and in part by the National Research Foundation of Korea (NRF) grant funded by the Korea government (MSIT) under Grant 2019R1A2C2085189. Recommended for publication by Associate Editor C. K. Tse. (*Corresponding author: Jeongjin Roh.*)

Jiho Moon and Jeongjin Roh are with the Department of Electrical Engineering, Hanyang University, Ansan 15588, South Korea (e-mail: roto92@hanyang.ac.kr; jroh@hanyang.ac.kr).

Jaeseong Lee and Jupyo Hong are with the LX Semicon Corporation, Yuseong 34027, South Korea (e-mail: jaeseong509@lxsemicon.com; jphong@lxsemicon.com).

Khurram Javed is with the Department of Electrical Engineering, Institute of Space Technology, Islamabad 44000, Pakistan (e-mail: khurram.javed@mail.ist.edu.pk).

Color versions of one or more figures in this article are available at <https://doi.org/10.1109/TPEL.2023.3243303>.

Digital Object Identifier 10.1109/TPEL.2023.3243303

LEDs [9], [10], [11]. In terms of benefits, LED-based automotive headlights can improve visibility and contribute to driving safety. For example, by controlling individual LEDs in LED matrix headlights, glare can be reduced, or a specific signal can be sent to oncoming pedestrians or vehicles on the road. Various studies on LED matrix headlight systems have been conducted, and the system is gaining popularity in the industry [12], [13], [14], [15], [16], [17].

The LED matrix headlight systems were controlled using a dedicated LED matrix controller. Automotive headlights are not only important for driving but also ensure the safety of vehicles, passengers, and other road users. Therefore, state-of-the-art LED matrix controllers are necessary. Essentially, the luminous intensity of all the LEDs is regulated by the matrix controller, which also maintains a fixed level by keeping the current constant despite changes in the supply voltage or fluctuations caused by turning the LEDs ON and OFF.

Fig. 1(a) presents a block diagram of a conventional LED matrix headlight system [14], [15]. The system contains two dc–dc converters (for pre-boost control), a matrix manager (to control the LEDs), and a microcontroller that delivers signals received from the outside. The boost converter supply was from an automotive battery. Fig. 1(a) shows the input voltage range of automotive batteries [18], which experience extremely wide voltage variations owing to their use in the starting system and load dump conditions. Therefore, the dc–dc converter must be able to operate over a wide input voltage range.

An external headlight-control signal that determines the ON/OFF status of the LED is transmitted to the controller area network. Simultaneously, this signal is transmitted to the microcontroller through a transceiver. After receiving the signal, the microcontroller determines the appropriate output voltage for the required number of LEDs through serial peripheral interface communication with the dc–dc converter. Additionally, the microcontroller transmits a brightness control signal to the matrix manager through universal asynchronous receiver/transmitter communication. After receiving this brightness control signal, the matrix manager switches the individual LEDs ON or OFF using bypass switches.

The use of two power converters reduces the overall efficiency of the system, where the power conversion efficiency of the entire system is expressed as the product of the efficiencies of the individual boost and buck converters as  $\eta_{\text{total}} = \eta_{\text{boost}} \times \eta_{\text{buck}}$ . Because the total system efficiency is a product of two

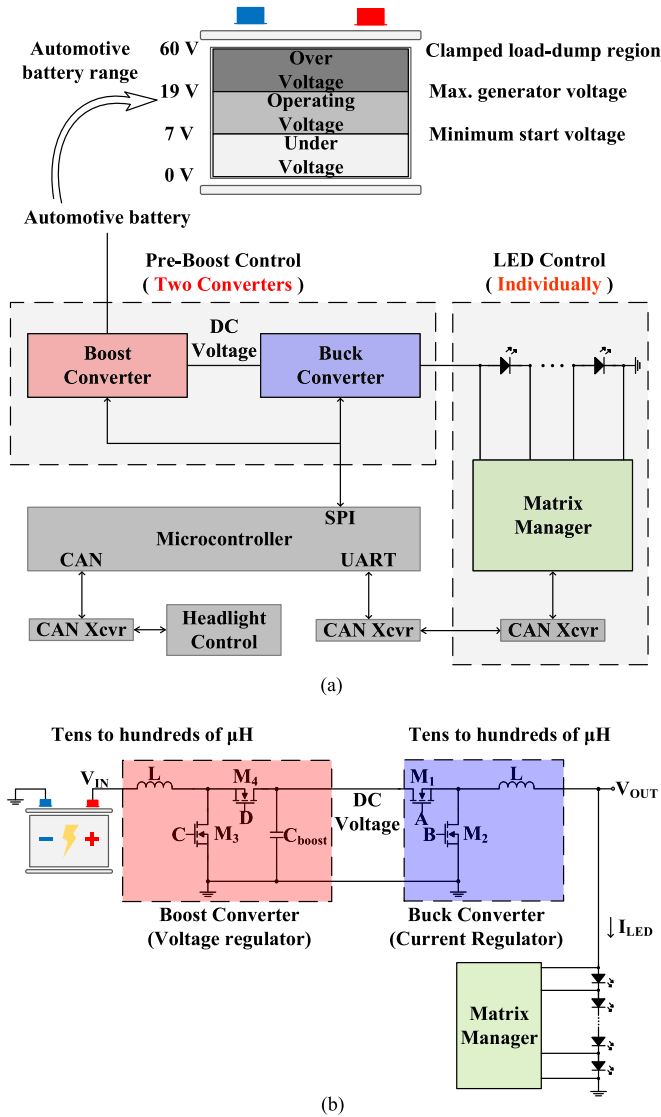


Fig. 1. Conventional LED matrix headlight system configuration. (a) Block diagram. (b) Schematic.

efficiencies, if the efficiency of either power converter is reduced, the total efficiency decreases considerably.

The circuit in Fig. 1(b) is a conventional power supply, which uses two inductive switching converters. The first is a boost converter (voltage regulator) that boosts the voltage from the battery, whereas the second is a buck converter (current regulator) that supplies current to the LEDs. If the automotive battery is directly connected to the buck current regulator without a boost converter, the wide voltage variations of the battery cannot provide the required input voltage to the buck converter. A capacitor ( $C_{boost}$ ) is required at the output terminal of the boost converter to provide a stable output voltage, whereas no output capacitor is required at the output terminal of the buck current regulator.

When a buck converter is used as the current regulator in the LED matrix headlight system, the current ripples in the inductor are transferred to the LEDs. To reduce this current ripple, the inductor should be at least in the order of tens of

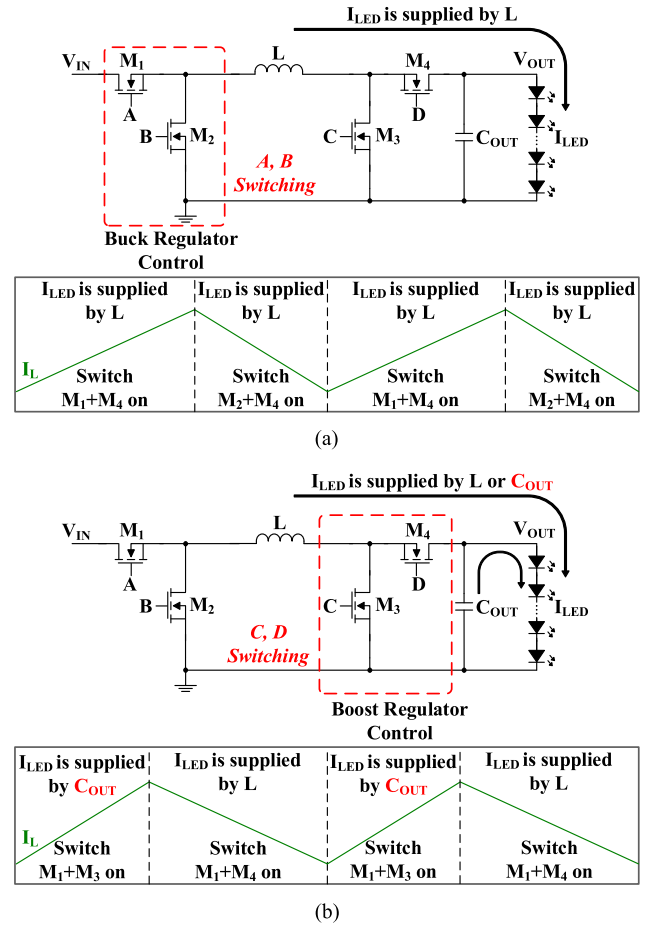


Fig. 2. Buck–boost converter comparison. (a) Buck mode. (b) Boost mode.

$\mu\text{H}$  [16] or even hundreds of  $\mu\text{H}$  in the case of industrial headlight applications [14], [15]. Because the typical LED matrix systems of headlights use two converters, the system efficiency is reduced. Moreover, multiple inductors are bulky and produce high electromagnetic interference levels [19].

There is no architecture in the literature for an automotive LED matrix system that uses only a single power converter. Moreover, conventional buck–boost converters cannot control LEDs individually because of the output capacitor.

Fig. 2 shows the reason for placing an output capacitor  $C_{OUT}$  in the buck–boost converter by demonstrating its operation in both the buck and boost modes. From Fig. 2(a), in the buck mode, signals A and B control transistors  $M_1$  and  $M_2$ , respectively. In this case, the load current ( $I_{LED}$ ) was continuously supplied by the inductor. Therefore, in the buck mode, the converter can operate as a current regulator with only a small (or no) output capacitor [20].

In the boost mode, signals C and D control transistors  $M_3$  and  $M_4$ , respectively, as depicted in Fig. 2(b). When transistor  $M_4$  is turned-ON, the load current is supplied by the inductor. However, when transistor  $M_3$  is ON, the output capacitor becomes the only means of supplying current. Therefore, it is necessary to use an output capacitor in the boost mode. As shown in Fig. 2(b), the current of the LED string can be supplied by the buck–boost converter because all LEDs in the string are turned-ON and -OFF

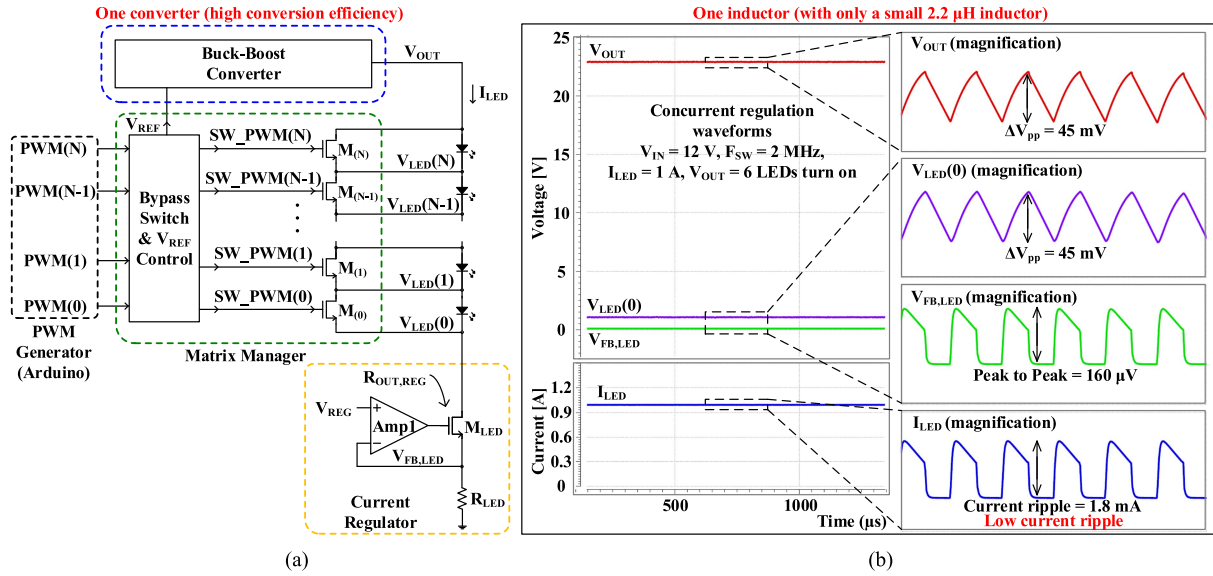


FIG. 3. Proposed architecture. (a) Structure. (b) Simulation results with concurrent current and voltage regulation waveforms.

simultaneously. Therefore, no voltage fluctuation occurs when the buck–boost converter is used as a power supply circuit.

Unlike LED strings, the individual ON/OFF operations of LEDs in a matrix system cause another issue when designing a power supply. The voltage across the LEDs can experience significant variations depending on the individual LED switching operations. Moreover, the output voltage of the converter should change instantaneously depending on the number of LEDs that are turned-ON. Because of the exponential nature of the diode current, if the voltage does not change rapidly, a large amount of current flows through the system. However, the transition time is not sufficiently short owing to the slow switching speeds and large output capacitance. Moreover, the large peak current affects the light intensity of LEDs and introduces long-term reliability concerns for the system.

This article presents a new buck–boost-based LED matrix system that uses the proposed concurrent current and voltage regulation scheme. In Section II, the details of the operation are explained, and the system implementation is presented in Section III. The measurement results are presented in Section IV. Finally, Section V concludes this article.

## II. PROPOSED ARCHITECTURE FOR CONCURRENT CURRENT AND VOLTAGE REGULATION

A block diagram of the proposed LED matrix system is shown in Fig. 3(a), which includes a current regulator that enables the individual control of LEDs without the requirement of two converters. The proposed architecture adjusts the output voltage (V<sub>OUT</sub>) of the buck–boost converter according to the number of LEDs in the on-state. Simultaneously, the current regulator prevents sudden current fluctuations through adaptive operation. The matrix manager in Fig. 3(a) includes bypass switches M<sub>(0)</sub>–M<sub>(N)</sub> that turn each LED ON or OFF. These switches are individually controlled by their corresponding pulsewidth modulation (PWM) signals, meaning that if a particular bypass

switch is turned-ON, the current flows through that switch. The voltage across the LED, which is parallel to the bypass switch, then approaches zero, turning the LED OFF.

The current regulator comprises a transistor (M<sub>LED</sub>), operational amplifier (Amp1), and resistor (R<sub>LED</sub>). The current regulator serves as the current source for the feedback operation. The amount of current flowing through the LEDs (I<sub>LED</sub>) can be determined using V<sub>REG</sub> and R<sub>LED</sub> and is given by  $I_{LED} = V_{REG} / R_{LED}$ . By selecting 100 mΩ and 100 mV for the R<sub>LED</sub> and V<sub>REG</sub>, respectively, the regulator is designed to sink 1.0 A.

When the bypass switch is turned-ON or -OFF, the voltage drop across the LED fluctuates significantly. Although the output of the buck–boost converter should follow the required voltage change, the slow response of the switching converter to charge or discharge the output capacitor causes the aforementioned current spike and long-term reliability issues.

The current regulator operates as a constant-current source circuit. The M<sub>LED</sub> operates as a common-source amplifier, which includes a degeneration resistor (R<sub>LED</sub>) and local negative feedback using a differential amplifier (Amp1). During the circuit operation, if a small amount of current increases through M<sub>LED</sub>, the voltage of the R<sub>LED</sub> (V<sub>FB,LED</sub>) increases as well. The negative input of Amp1 senses this change, and Amp1 forces the gate voltage of M<sub>LED</sub> to drop. Owing to the inverting amplification characteristic of the common-source circuit, M<sub>LED</sub> increases its drain voltage (V<sub>LED(0)</sub>). The output impedance (R<sub>OUT,REG</sub>) of the current regulator is defined as [21]

$$R_{OUT,REG} = r_o + (A_1 + 1)g_m r_o R_{LED} + R_{LED} \quad (1)$$

where  $r_o$  is the output resistance,  $g_m$  is the transconductance of M<sub>LED</sub>, and  $A_1$  is the gain of Amp1. During LED ON/OFF operations, if a current spike (ΔI) is generated, it is multiplied by R<sub>OUT,REG</sub> to produce a voltage. The instantaneous voltage change (ΔV) is defined as  $\Delta V = \Delta I \times R_{OUT,REG}$ . The drain voltage of the current regulator (V<sub>LED(0)</sub>) reacts to the current spike to maintain a constant I<sub>LED</sub>.

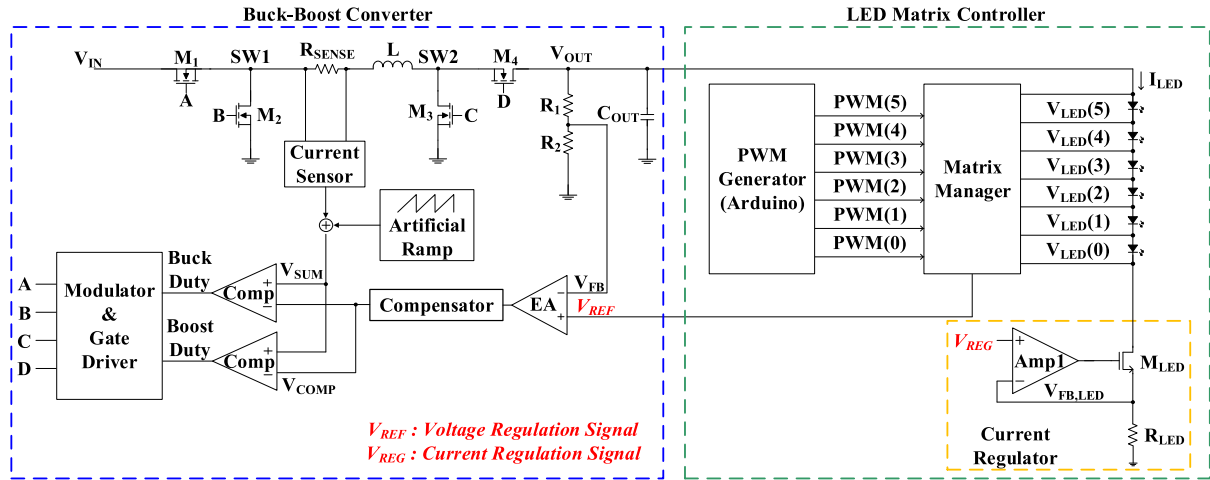


Fig. 4. LED matrix system for automotive headlights.

The combination of switching power converters and linear voltage regulators has previously been employed for envelope tracking in RF power amplifiers [22], [23], [24]. However, switching power converters are generally too slow to effectively control the output voltage and cannot meet the high-speed requirements of envelope tracking. Accordingly, linear voltage regulators are combined with the switching power converters to support fast variations in the output voltage of the system. In the proposed scheme, a current regulator (instead of a voltage regulator) is combined with a single power converter to improve the speed of operation of the LED matrix headlights, as displayed in Fig. 3(a). The proposed current regulator focuses on maintaining a fixed LED current, while previous studies on RF amplifiers have focused on fast control of the supply voltage.

Fig. 3(b) shows concurrent regulation simulation waveforms. The simulations were conducted by setting  $V_{IN} = 12$  V,  $F_{SW} = 2$  MHz, and  $I_{LED} = 1$  A, under the condition that the six LEDs were on at the output of the power converter. The proposed LED matrix headlight system regulated the current even with a small  $2.2 \mu\text{H}$  inductor. As shown in Fig. 3(b),  $V_{OUT}$  and  $V_{LED(0)}$  generate the same fluctuations ( $\Delta V_{pp} = 45$  mV) during the switching operation, and  $I_{LED}$  exhibited a ripple of only 1.8 mA. This represents a variation of less than 0.2% of  $I_{LED}$ .

### III. LED MATRIX SYSTEM IMPLEMENTATION

Fig. 4 depicts the overall architecture proposed in this article, which is mainly divided into a buck–boost converter and an LED matrix controller. The main control circuit of the buck–boost converter was designed and integrated into a semiconductor IC. The discrete components (inductor  $L$ , capacitor  $C_{OUT}$ , sense resistor  $R_{SENSE}$ , and four power transistors  $M_1$ – $M_4$ ) were fabricated on a printed circuit board (PCB). The LED matrix controller comprises a PWM generator, matrix manager, and current regulator. The PWM generator is implemented using an Arduino microcontroller board. The matrix manager receives signals from the PWM generator and then controls the individual

LEDs to be either ON or OFF. It also generates a  $V_{REF}$  signal that is used as a reference voltage for the buck–boost converter.

#### A. Buck–Boost Converter

The buck–boost converter shown in Fig. 4 was designed to achieve four modes: buck, (step-down) buck–boost, (step-up) buck–boost, and boost modes [25]. Owing to this four-mode operation, it is possible to prevent abrupt duty changes in mode conversion and minimize the inductor current ripple [26]. The error amplifier (EA) subtracts the  $V_{FB}$  signal from the  $V_{REF}$  signal. A compensation circuit is employed to ensure the stability of the feedback loop. Therefore, the  $V_{COMP}$  signal, which is required to generate the duty cycle of the buck–boost converter, can be obtained. Additionally, because the current-mode control method is used [27], the current flowing through the inductor can be sensed via the voltage drop across the  $R_{SENSE}$  resistor. When performing the current sensing operation, a common mode fluctuation occurs in the switching operation of the buck–boost converter. This common-mode noise effect is reduced using a transconductance amplifier with degeneration resistors [25]. The duty-controlled A, B, C, and D signals were used to turn the four power transistors  $M_1$ – $M_4$  ON and OFF to regulate the output voltage. The feedback voltage  $V_{FB}$  follows the reference voltage  $V_{REF}$  generated by the matrix manager. More specifically, the output voltage of the buck–boost converter is controlled by the matrix manager. The matrix manager adaptively controls  $V_{REF}$  depending on the number of turned-ON LEDs. Within the circuit,  $V_{REF}$  is a key signal that is responsible for voltage regulation, whereas  $V_{REG}$  is another key signal for the current regulator that is responsible for current regulation.

#### B. LED Matrix Controller

Fig. 5 presents the simulated voltage and current waveforms when the LEDs were turned-ON and -OFF, respectively. Here,  $V_{LED(0)}$  represents the drain voltage of  $M_{LED}$  and  $V_{OUT} - V_{LED(0)}$  represents the voltage drop across the six LEDs. When a bypass switch is activated to turn-OFF an LED, the output voltage of

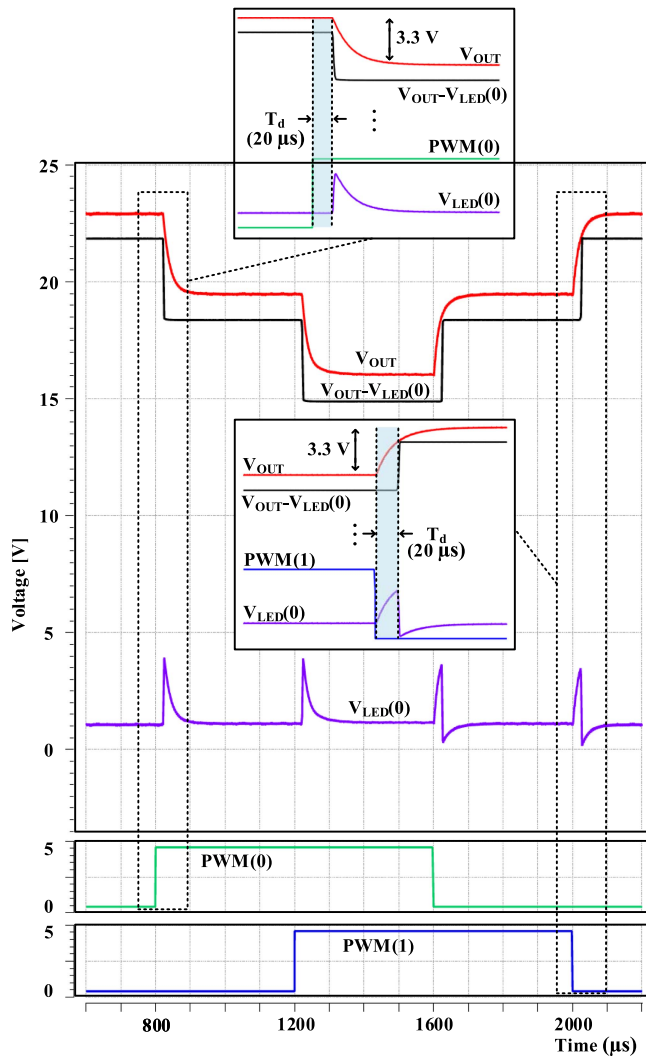


Fig. 5. LED turn-ON/OFF waveforms.

the buck-boost converter takes time to change. The overall voltage drop across the LEDs cannot change immediately if there is no current-regulation scheme. Therefore, during this transition time, the remaining turned-ON LEDs may experience a higher voltage across each LED. This introduces a large current spike owing to the exponential nature of diodes. To prevent this undesirable effect, the drain voltage of  $M_{LED}$  (i.e.,  $V_{LED}(0)$ ) is instantaneously increased via the current regulator. This increased drain voltage immediately reduces the overall voltage drop across the LEDs ( $V_{OUT}-V_{LED}(0)$ ), maintaining identical voltages across the individual LEDs. The buck-boost converter then slowly reduces the output voltage, and the current regulator reduces  $V_{LED}(0)$  to the previous voltage.

When an LED is turned-ON by turning-OFF the bypass switch, the overall voltage drop across the LEDs must immediately increase to maintain the same voltage level across the individual LEDs. If the output voltage of the buck-boost converter does not increase before the LED is turned-ON, the current decreases significantly because of the reduced individual LED voltage levels. The decreased current implies that the brightness of

the LED was also reduced. Therefore, to control the overall LED voltage ( $V_{OUT}-V_{LED}(0)$ ) during LED operation, the buck-boost converter increases the output voltage ( $V_{OUT}$ ) in advance. For smooth operation, the  $V_{REF}$  signal was increased before turning-ON the LED. Simultaneously, when the LED turns ON, the previously increased  $V_{OUT}$  and fast operation of the current regulator minimize any current fluctuations.

When several LEDs are turned-ON simultaneously, a power converter is required to increase the output voltage in steps of more than 10 or 20 V, depending on the number of LEDs turned-ON. However, this sudden voltage increase causes the inrush current to charge the output capacitor of the power converter and degrades the long-term reliability. This phenomenon is similar to the situation during start-up [28]. The soft-start circuit prevents inrush current. Similarly, the sequential control of the PWM signals (see Fig. 5) prevent any inrush current by sequentially turning the LEDs ON or OFF with a predetermined time delay.

### C. Bypass Switch and $V_{REF}$ Controller

The reference voltage ( $V_{REF}$ ) is required to control the buck-boost converter and is generated by the circuit shown in Fig. 6(a). This adaptive  $V_{REF}$  signal helps control  $V_{OUT}$  to a voltage that matches the forward bias voltage of the number of LEDs that are turned-ON. In this article, six LEDs were used for design and testing. When  $PWM(x)$  is applied to the control logic, a time-delayed signal  $SW\_PWM(x)$  is generated, where  $x$  refers to a number between 0 and 5. The generated signal is used to drive the bypass switch in Fig. 3(a) and set the SR latch. Similarly, when  $PWM(x)$  becomes low, the  $reset(x)$  signal is activated during the  $T_d$  delay time, resulting in  $V_F(x)$  becoming low, as shown in Fig. 6(b). When the bypass switches are turned-OFF, the drain voltage of the  $M_{LED}$  in Fig. 3(a) instantaneously drops to secure the necessary voltage across the activated LED. If this voltage drop places the  $M_{LED}$  into a deep triode region, the feedback gain and speed of the current regulator will be significantly reduced. This would degrade the performance of the current regulator, meaning that a constant current could not be maintained. To overcome this performance degradation, a delay time  $T_D$  was implemented in the control logic, allowing the  $reset(x)$  signal to be generated in advance before turning-OFF the bypass switch. Because the output of the SR latch ( $V_F(x)$ ) is connected to the PMOS switch of the  $V_{REF}$  generator, it operates as an active low signal. Specifically,  $V_F(x)$  is reduced in advance, increasing  $V_{LED}(0)$  before the bypass switch is turned-OFF.

The current regulator has a sufficient voltage margin to control the current when the bypass switch turns OFF. Six  $V_F(x)$  signals were used to control the amount of current flowing through  $R_{REF}$ . When all LEDs are ON,  $V_{REF}$  can be expressed by the following equation:  $V_{REF} = I_{REF} \times R_{REF}$ , where  $I_{REF} = I_{M0} + I_{M1} + \dots + I_{M5}$ .

The generated  $V_{REF}$  signal goes to the buck-boost converter, as shown in Fig. 4. The reference voltage controls the output voltage of the power converter according to the number of turned-ON LEDs, ensuring the optimum power efficiency of the LED matrix system. Using the bypass switch and  $V_{REF}$

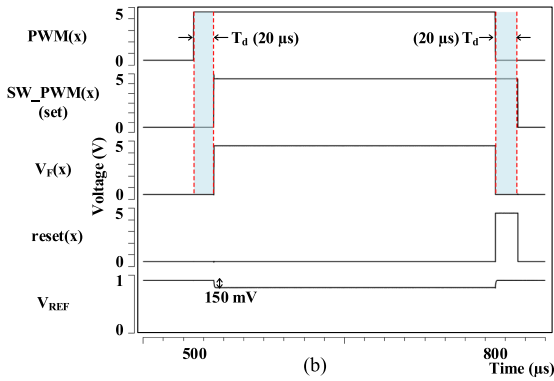
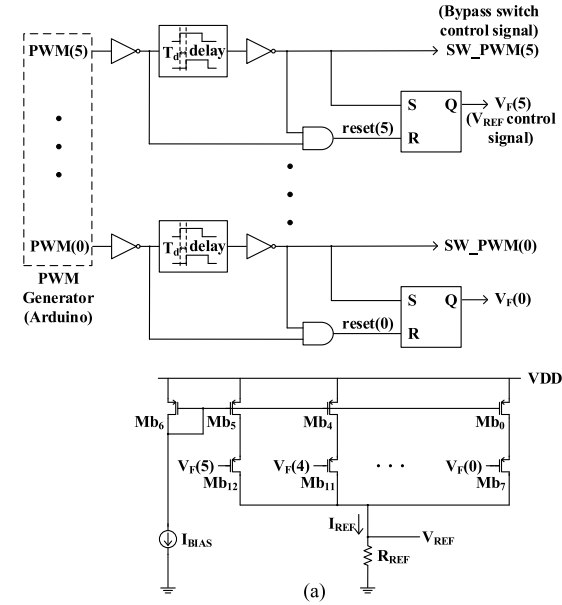


Fig. 6. Bypass Switch and  $V_{REF}$  Controller. (a) Simplified signal generator. (b) simulated waveforms.

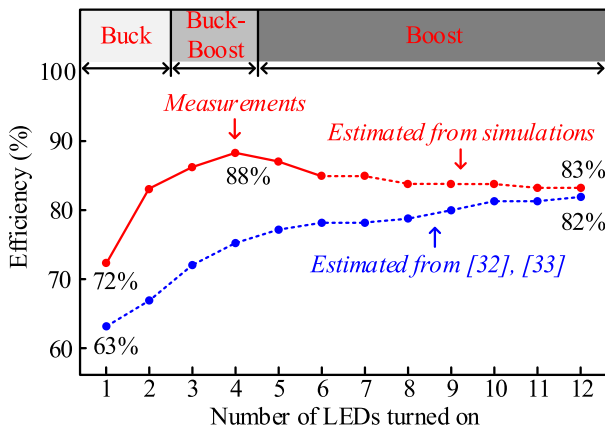


Fig. 7. Efficiency comparison.

control method, a single buck–boost converter can perform stable concurrent regulation. Compared to conventional topologies that combine the voltage regulation of the boost converter and the current regulation of the buck converter, the proposed system has clear advantages. For example, the proposed LED

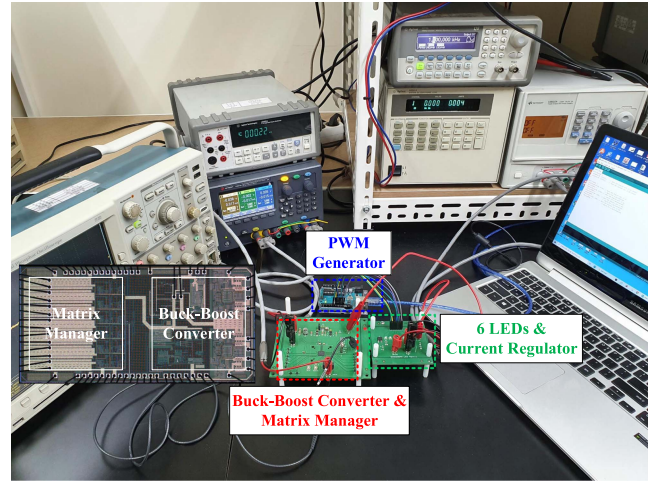


Fig. 8. Experimental hardware prototype.

matrix headlight system is expected to have increased efficiency owing to its single buck–boost converter. Additionally, the total PCB area can be reduced because only one inductor is required.

The LED forward bias voltage varies depending on external factors such as the amount of current flowing through the LED, temperature, and aging. By comparison,  $V_{OUT}$  can be controlled by changing  $V_{REF}$ . During the ON/OFF operation of the LEDs,  $V_{REF}$  is transmitted to the buck–boost converter to set  $V_{OUT}$ , as shown in Fig. 4. However, the errors between the LED forward bias voltage and  $V_{OUT}$  can affect the performance of the proposed LED matrix headlight system. This could reduce the efficiency of the system and cause problems in the current control mechanism. Therefore, it is necessary to provide an optimum  $V_{OUT}$  for the LEDs. Generally, power converter design with varying LED characteristics (owing to temperature variations and aging) has been an issue within the industry. A common solution is to monitor the LEDs using an analog-to-digital converter and trim the output voltage using a microcontroller [29]. Although this monitoring system is not implemented herein, this conventional monitoring and trimming scheme can be applied to provide an optimum supply for the proposed LED matrix headlight system to cope with varying LED characteristics.

Another concern in achieving an optimum  $V_{OUT}$  level is the accuracy of the  $V_{REF}$  generation circuit itself. The bias current ( $I_{BIAS}$ ) in Fig. 6(a) is generated from a bandgap reference circuit, which can generate an accurate bias voltage and current with less than 1% variation over a wide temperature range [30]. Accurate matching of the current mirrors in Fig. 6(a) can also be achieved using complementary metal-oxide-semiconductor (CMOS) layout techniques, such as the common-centroid scheme [21], [31].

The red graph in Fig. 7 shows the efficiency of the proposed LED matrix system, calculated using an input voltage of 12 V, which is the nominal voltage of an automotive battery. As the number of LEDs increased, the output voltage of the converter increased. The red graph displays the efficiency of the proposed buck–boost system experiencing all four operation modes with the number of turned-ON LEDs.

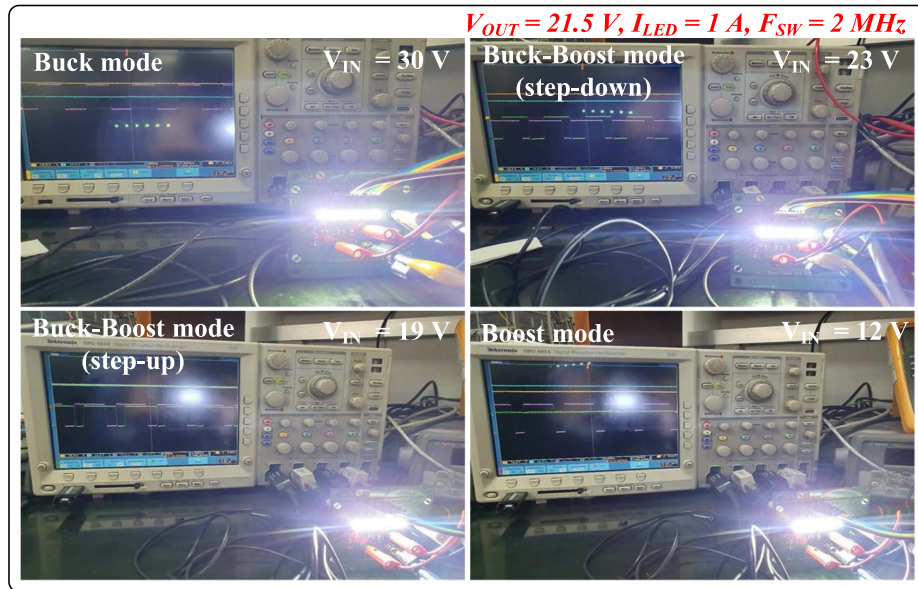


Fig. 9. Demonstrations of the proposed system.

The operation modes are also displayed in Fig. 7. The buck–boost mode includes both the (step-down) buck–boost and (step-up) buck–boost modes, which are used when the input and output voltage levels are relatively close. The hysteresis of the mode selection circuit determines the mode and prevents toggling of the modes, which could generate unpredictable output voltage noise [25].

From the figure, it is evident that the efficiency varies with the mode changes. If only one LED is turned-ON, the power converter operates in buck mode, whereas when the number of turned-ON LEDs increases, the converter operates in both buck–boost and boost modes. With only one LED, the efficiency decreases owing to the power losses in the current regulator. In contrast, as the LEDs turn-ON, power losses in the current regulator constitute only a small portion of the total power losses; hence, the efficiency increases. Because the prototype chip was fabricated with six bypass switches for the matrix manager, the efficiency of the proposed system with up to six LEDs was obtained from experimental measurements. The efficiencies of seven (or more) LEDs were estimated through simulations.

The blue graph in Fig. 7 shows the estimated efficiency referencing information from [14]. Using the typical automotive battery voltage of 12 V, the boost converter was assumed to generate a boosted voltage of 48 V [14], [16]. The buck converter then provides regulated current to the LEDs. The efficiency of the boost converter, was assumed to be 90%, which was estimated from [32]. The efficiency of the buck converter was referenced from [33] using the duty cycle conditions. Particularly, when a small number of LEDs were turned-ON, the proposed system achieved a significant efficiency advantage.

#### IV. MEASUREMENT RESULTS

Fig. 8 displays the experimental hardware prototype used to verify the proposed architecture, which consists of two PCBs

TABLE I  
EXPERIMENTAL SPECIFICATIONS

Symbol	Quantity
Input voltage $V_{IN}$	7–60 V
Output voltage $V_{OUT}$	1.05–60 V
LED current (max) $I_{LED}$	2.0 A
Switching frequency $F_{SW}$	2.0 MHz
Peak efficiency	91%
Power switches $M_1$ – $M_4$	BUK9M42-60E
Power inductor $L$	2.2 $\mu$ H
Output capacitor $C_{OUT}$	5 $\mu$ F
PWM generator	Arduino Uno R3
LED	XPEWHT-L1-R250-00D01

and an Arduino microcontroller board (PWM generator). One PCB was used to test the designed buck–boost converter and matrix manager chip, whereas the other contained the LEDs and current regulator. The Cree XLamp LEDs were connected in series on the PCB, and the current regulator was implemented using discrete components and an operational amplifier.

The buck–boost converter and matrix manager in Fig. 3(a) are implemented as a semiconductor chip using a 0.18- $\mu$ m BCD process. An Arduino board was used to generate the duty-controlled PWM signals by programming the microcontroller chip. Table I presents a summary of the system and components used in the hardware prototype.

Fig. 9 demonstrates the proposed system. The switching frequency of the buck–boost converter was set to 2 MHz with

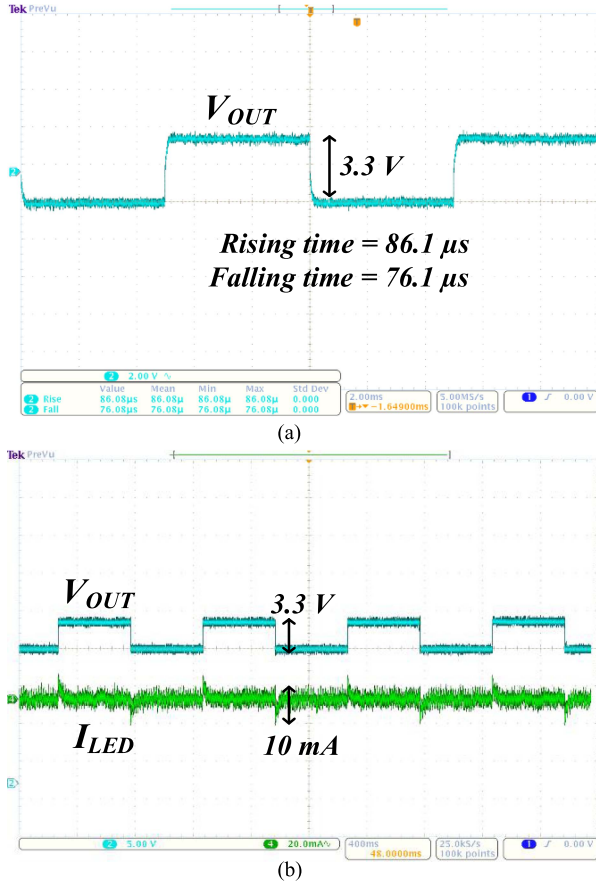


Fig. 10. Measurement results of (a)  $V_{OUT}$  during LED ON/OFF and (b) current regulation for  $I_{LED} = 1 \text{ A}$ .

$I_{LED} = 1 \text{ A}$ , and the input voltage was changed to test the operation of the system. The four operation modes of the designed buck–boost converter were verified, and the LED matrix system operated well in all four modes, as expected.

The waveforms in Fig. 10 display the output voltage of the buck–boost converter ( $V_{OUT}$ ). When the LED is turned-ON and -OFF periodically, the output voltage changes according to the ON/OFF operation. The output voltage followed the optimum LED voltage through the feedback control of the power converter. The required rising and falling times of the output voltage were measured as 86.1 and 76.1  $\mu\text{s}$ , respectively. The current variations were also measured during the ON/OFF operation. The current regulator minimized current fluctuations, and a small spike of only 10 mA was observed. This current variation was only 1% of the designated LED current.

Fig. 11 shows the waveform of the output voltage when the three bypass switches are turned-ON and -OFF. The measurement was performed at an input voltage of 30 V with  $I_{LED} = 1.0 \text{ A}$ . Three PWM signals were generated and applied to the matrix to control the bypass switches. The variation in  $V_{OUT}$  was measured, and the output voltage was changed according to the PWM signals (as expected).

Dimming tests are performed using the proposed system, as shown in Fig. 12. For comparison, LED1 (in the middle) was set to the maximum brightness for all five dimming tests. It

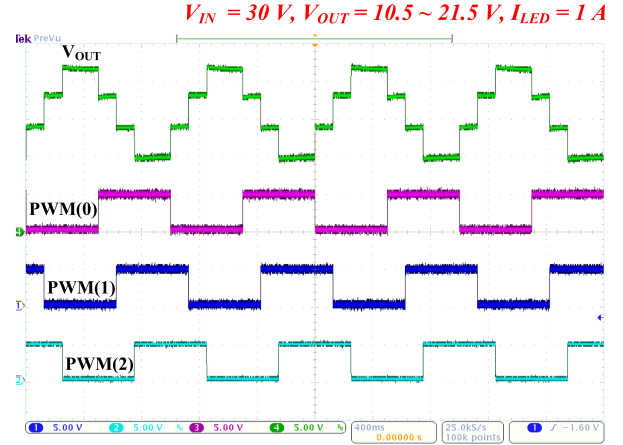


Fig. 11. PWM measurement results.



Fig. 12. LED matrix dimming tests.

should be noted that the brightness of the middle LED appeared different in the pictures because of the automatic brightness control of the digital camera, whereas the actual brightness was identical to that of the human eyes in the test room. The bottom LED (LED0) underwent actual dimming. For the dimming of LED0, 1%, 10%, 50%, 90%, and 99% (from left to right) of the PWM duty signal was applied, and accurate brightness control was observed in the test room.

## V. CONCLUSION

Herein, an efficient power-conversion architecture was proposed for automotive LED matrix headlights. The proposed system used only one power converter for the LED matrix, whereas the conventional systems require two power converters. Moreover, a concurrent regulation scheme means that the system uses only one power converter with a small inductor. The proposed architecture improves the efficiency of the overall system while regulating a uniform LED current, even when the LEDs turn-ON and -OFF. The prototype system was demonstrated using automotive LED lamps, where successful operation was observed and measured.

## REFERENCES

- [1] D. Gacio, J. Cardesin, E. L. Corominas, J. M. Alonso, M. Dalla-Costa, and A. J. Calleja, "Comparison among power LEDs for automotive lighting applications," in *Proc. IEEE Ind. Appl. Soc. Annu. Meeting*, Edmonton, AB, Canada, 2008, pp. 1–5.



- [2] A. Pollock, H. Pollock, and C. Pollock, “High efficiency LED power supply,” *IEEE J. Emerg. Sel. Topics Power Electron.*, vol. 3, no. 3, pp. 617–623, Sep. 2015.
- [3] Y. Zhang, G. Rong, S. Qu, Q. Song, X. Tang, and Y. Zhang, “A high-power LED driver based on single inductor-multiple output DC–DC converter with high dimming frequency and wide dimming range,” *IEEE Trans. Power Electron.*, vol. 35, no. 8, pp. 8501–8511, Aug. 2020.
- [4] E. Lee, B. Choi, D. Nguyen, B. Choi, and C. Rim, “Static regulated multistage semiactive LED drivers for high-efficiency applications,” *IEEE Trans. Power Electron.*, vol. 31, no. 9, pp. 6543–6552, Sep. 2016.
- [5] M. Tahan and T. Hu, “Multiple string LED driver with flexible and high-performance PWM dimming control,” *IEEE Trans. Power Electron.*, vol. 32, no. 12, pp. 9293–9306, Dec. 2017.
- [6] M. Marina, M. Perdigo, A. S. Mendes, R. Pinto, and J. Alonso, “Analysis, design, and experimentation of a dimmable resonant-switched-capacitor LED driver with variable inductor control,” *IEEE Trans. Power Electron.*, vol. 32, no. 4, pp. 3051–3062, Apr. 2017.
- [7] C. S. Wong, K. H. Loo, Y. M. Lai, M. L. Chow, and C. Tse, “An alternative approach to LED driver design based on high-voltage driving,” *IEEE Trans. Power Electron.*, vol. 31, no. 3, pp. 2465–2475, Mar. 2016.
- [8] R. Sangrody, M. Poursmaeil, M. Marzband, and E. Poursmaeil, “Resonance-based optimized buck LED driver using unequal turn ratio coupled inductance,” *IEEE Trans. Power Electron.*, vol. 35, no. 12, pp. 13068–13076, Dec. 2020.
- [9] M. Khatua et al., “High-performance megahertz-frequency resonant DCDC converter for automotive LED driver applications,” *IEEE Trans. Power Electron.*, vol. 35, no. 10, pp. 10396–10412, Oct. 2020.
- [10] V. K. S. Veeramallu, S. Porpandiselvi, and B. L. Narasimharaju, “A non-isolated wide input series resonant converter for automotive LED lighting system,” *IEEE Trans. Power Electron.*, vol. 36, no. 5, pp. 5686–5699, May 2021.
- [11] S. Mukherjee, V. Yousefzadeh, A. Sepahvand, M. Doshi, and D. Maksimovic, “A two-stage automotive LED driver with multiple outputs,” *IEEE Trans. Power Electron.*, vol. 36, no. 12, pp. 14175–14186, Dec. 2021.
- [12] M. Waldner and T. Bertram, “Evaluation of the light distribution of a matrix-headlight with a hardware-in-the-loop-simulation,” in *Proc. 13th Int. Symp. Automot. Lighting*, 2019, pp. 1311–1316.
- [13] M. Waldner, M. Krämer, and T. Bertram, “Digitization of matrix-headlights that move as in the real test drive,” in *Proc. IEEE/ASME Int. Conf. Adv. Intell. Mechatronics*, 2020, pp. 264–269.
- [14] Texas Instruments, “TPS92661-Q1 high-brightness LED matrix manager for automotive headlight systems,” 2014. [Online]. Available: <https://www.ti.com/product/TPS92661-Q1>
- [15] NXP Semiconductors, *System solutions for intelligent automotive exterior lighting*, 2019. [Online]. Available: <https://community.nxp.com/t5/Connects-Training-Material/ADAS-LED-Drivers-and-Matrix-LED-Controller-for-Auto-Exterior/ta-p/1117788>
- [16] Analog Devices, *MAX20092 Eval. Syst.*, 2018. [Online]. Available: <https://www.maximintegrated.com/en/products/power/led-drivers/MAX20092EVSYS.html>
- [17] W. Jeon, S. Hwang, J. Kim, and M. Lee, “Active-matrix Pixelated-LED control system for automotive headlamps,” *IEEE Access*, vol. 10, pp. 45553–45561, 2022.
- [18] A. Baschiroto, P. Harpe, and K. Makinwa, *Wideband Continuous-Time  $\Sigma \Delta$  ADCs, Automotive Electronics, and Power Management*, Berlin, Germany: Springer, 2017.
- [19] Y. Qu, W. Shu, and J. S. Chang, “A Low-EMI, high-reliability PWM-Based dual-phase LED driver for automotive lighting,” *IEEE J. Emerg. Sel. Topics Power Electron.*, vol. 6, no. 3, pp. 1179–1189, Sep. 2018.
- [20] W. Yang, H. Yang, C. Huang, K. Chen, and Y. Lin, “A high-efficiency single-inductor multiple-output buck-type LED driver with average current correction technique,” *IEEE Trans. Power Electron.*, vol. 33, no. 4, pp. 3375–3385, Apr. 2018.
- [21] B. Razavi, *Design of Analog CMOS Integrated Circuits*, 2nd ed. New York, NY, USA: McGraw-Hill, 2015.
- [22] P. F. Miaja, J. Sebastián, R. Marante, and J. A. García, “A linear assisted envelope amplifier for a UHF polar transmitter,” *IEEE Trans. Power Electron.*, vol. 29, no. 4, pp. 1850–1861, Apr. 2014.
- [23] Y. Li, X. Ruan, Y. Wang, and C. Zhang, “Hysteresis voltage prediction control for multilevel converter in the series-form switch-linear hybrid envelope tracking power supply,” *IEEE Trans. Power Electron.*, vol. 35, no. 12, pp. 13663–13672, Dec. 2020.
- [24] J. Rodríguez, J. R. García-Meré, D. G. Aller, and J. Sebastián, “Pulsewidth modulated three-level buck converter based on stacking switch-cells for high power envelope tracking applications,” *IEEE Trans. Power Electron.*, vol. 37, no. 5, pp. 5786–5800, May 2022.
- [25] J. Moon et al., “60-V non-inverting four-mode BuckBoost converter with bootstrap sharing for non-switching power transistors,” *IEEE Access*, vol. 8, pp. 208221–208231, 2020.
- [26] N. Zhang, G. Zhang, and K. See, “Systematic derivation of dead-zone elimination strategies for the noninverting synchronous buck–boost converter,” *IEEE Trans. Power Electron.*, vol. 33, no. 4, pp. 3497–3508, Apr. 2018.
- [27] R. W. Erickson and D. Maksimovic, *Fundamentals of Power Electronics*, 2nd ed. Norwell, MA, USA: Kluwer, 2001.
- [28] Texas Instruments, *Des. High-Perform., Low-EMI Automot. Power Supplies*, 2017. [Online]. Available: <https://www.ti.com/lit/snva780>
- [29] Texas Instruments, *LED Temp. Protection by Vf Monit.*, 2019. [Online]. Available: <https://www.ti.com/lit/slvaeb5>
- [30] P. R. Gray, P. J. Hurst, S. H. Lewis, and R. G. Meyer, *Analysis and Design of Analog Integrated Circuits*, 5th ed. Hoboken, NJ, USA: Wiley, 2009.
- [31] A. Hasting, *The Art of Analog Layout*. Englewood Cliffs, NJ, USA: Prentice-Hall, 2001.
- [32] Texas Instruments, *LM5157x-Q1 2.2-MHz Wide  $V_{IN}$  50-V Boost/SEPIC/Flyback Converter with Dual Random Spread Spectrum*, 2021. [Online]. Available: <https://www.ti.com/product/LM5157-Q1>
- [33] Texas Instruments, *LM3409, -Q1, LM3409HV, -Q1 P-FET buck controller for high-power LED drivers*, 2016. [Online]. Available: <https://www.ti.com/product/LM3409>